Breaking, Making, and Twisting of Chemical Bonds in Gas, Liquid, and Nanocavities

ABDERRAZZAK DOUHAL†

Departamento de Química Física, Sección de Químicas, Facultad de Ciencias del Medio Ambiente, Campus Tecnológico de Toledo, Avenida Carlos III, SN, Universidad de Castilla-La Mancha, 45071 Toledo, Spain

Received October 31, 2003

ABSTRACT

In this Account, we recount on our studies of 1′-hydroxy-2′-acetonaphthone (HAN, a proton transfer prototype molecule) in gas, solutions, and nanocavities. The internal H-bond photoreaction in HAN leads to a keto type structure, and following its formation, an internal twisting motion gives birth to keto rotamers. Theory, temperature, and solvent effects on its photodynamics show the involvement of efficient radiationless processes in both keto structures. When HAN is caged in a cyclodextrin nanocavity, the spectroscopy, photodynamics, and issues of twisting motion are strongly affected and could be tuned: a behavior relevant to those of many chemical and biological systems.

Introduction

In molecular science, the essence of chemical reactivity and therefore the change of matter is due to electron exchange, the breaking, making, and rotating of chemical bonds.[1−9] The driving force behind these elementary processes comes from induced orbital interactions giving rise to atomic charge redistribution and thus to swings in acidity (or basicity) or in electronic affinity (or ionization potential) of the involved atoms, groups, or molecules. Since Mulliken, Lewis, and Pauling, much progress has and is being made for understanding the potential-energy surfaces (PES) that govern the dynamics of a chemical reactivity in gas, cluster, and condensed phases. A particular case is the H-bond, and because of its special unique character (energy, directionality, and quantum tunneling) and the related ubiquitous phenomena in influencing architectural, energetic, and dynamical aspects of a wide variety of systems ranging from material to life sciences, the related proton (or H-atom) transfer is one of the most important studied reactions.[10−16] Furthermore, the H-bond breaking and making processes can trigger other chemical bond events such as cis−trans isomerization found in retinal proteins for example. In addition to that, molecules undergoing proton transfer have been suggested as an active medium in lasing devices and as fast systems for logic gates[17] and molecular memory.[18] Others systems have been used for probing the topology of nanocavities[19,20] and for detecting metals,[21,22] to cite a few examples.

Scheme 1. Structures of Enol (E*), Keto (K*), and Keto Rotamer (KR*) of 1′-Hydroxy-2′-acetonaphthone (HAN) at the S_1 State with the Arrows Showing the Involved Atomic Motion

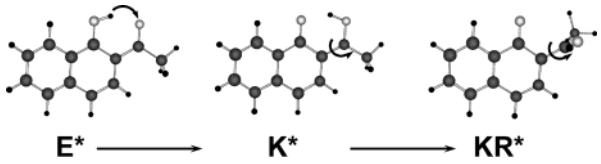

A prototype system showing proton transfer and twisting motion following an electronic excitation is 1′-hydroxy-2′-acetonaphthone (HAN).[23−34] It is an aromatic molecule with two groups able to form an intramolecular H-bond (Scheme 1). This bond is comparable to that in methyl salicylate[35−39] but with a larger π electronic molecular system. HAN has been studied from the point of view of theory (quantum chemistry) and experiment: gas, liquid, and nanocavity phases. Here, we recount our results of studying HAN[23,24,29−34] aiming at a unified picture of the photophysical events following a photoinduced excitation of this type of molecule undergoing fast proton transfer and twisting motion of the protonated group. We believe that the results are relevant to the behavior of several molecular systems undergoing proton-transfer reactions. In the following, we will discuss the results of ab initio calculations, dispersed emission under jet-cooled molecular beam conditions, and temperature, solvent, and nanocavity effects on the fluorescence and dynamics of HAN. Details can be found in the original contributions.[23,24,29−34]

Theoretical Studies

The ab initio theoretical calculations have shown that, at the S_0 state, the enol (E) form is the most stable structure and it has an intramolecular H-bond between the OH and the CO groups (Scheme 1).[29] The keto (K) type structure result of an intramolecular proton transfer in E does not have a local minimum at S_0. However, other local minima due to rotation of OH and acetyl groups or protonated acetyl group (keto type rotamer, KR) exist at S_0 (Figure 1).[29] These structures might be accessible through electronic or vibrational excitation of E. Following an electronic excitation, the behavior of HAN is completely different from that at S_0.[30] The internal H-bond in the excited enol (E*) is stronger. From the point of view of geometry, the excited E shows a shortening of the O···O distance (2.56 Å) by 0.03 Å. This is also reflected by an increase in acidity and in basicity of the OH and $CO(CH_3)$ groups (necessary for the subsequent transfer of proton or H-atom), respectively. The $CO(CH_3)$ increases its elec-

Abderrazzak Douhal, born in 1959, was educated in Beni Mellal (Morocco). He received his Ph.D. degree from Université Kadi Ayyad (Marrakesh) after working on solvation and photoinduced proton-transfer reactions at the same university and at the Institute of Physical Chemistry "Rocasolano" (CSIC, Madrid). After a 2-year postdoctoral research position at the Institute of Molecular Science (Okazaki, Japan) working on ultrafast reactions as a fellow of the Japanese Ministry of Education, Science, and Culture and the JSPS, he joined in 1992 the "Laboratoire de Photophysique Molecular" at Orsay (CNRS-University of Paris-Sud), and later he moved to the University of Castilla-La Mancha (Toledo, Spain). He was a visiting researcher at the California Institute of Technology for several periods to work with Professor A. H. Zewail. His current research focuses on ultrafast dynamics in nanostructures.

† E-mail: abderrazzak.douhal@uclm.es. Fax: + 34-925-268840.

10.1021/ar030247b CCC: $27.50
Published on Web 04/17/2004

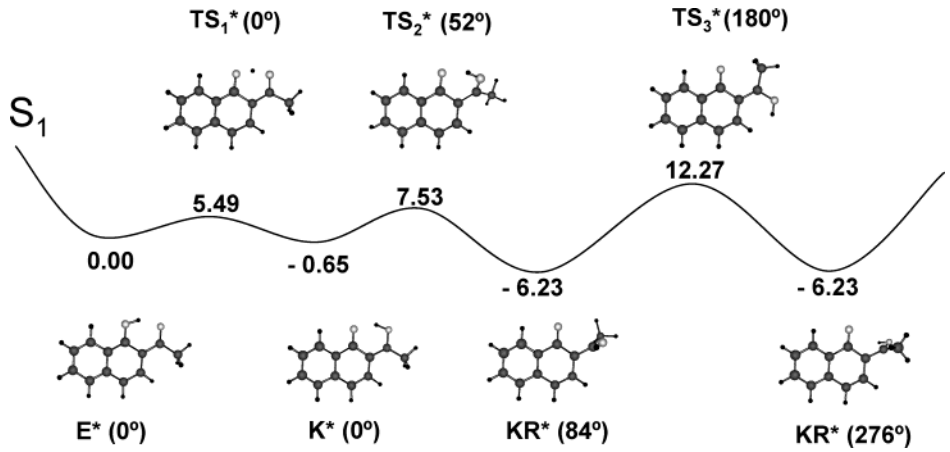

FIGURE 1. Energy profile for proton motion within E* and twisting motion of formed K* to give KR* at the S_1 state. Energies (kcal/mol) are relative to that of E*. Between parentheses are the value of the dihedral angle between the planes of acetyl group and naphthalenic frame.

tronic charge by 0.07 e, while those of the carbon atom bringing the OH and $CO(CH_3)$ suffer a loose of about 0.05 e. The ultrafast electronic redistribution helped by vibrational motions constitutes the driving force for the proton transfer. According to the calculations the origin of the energy barrier for the proton transfer in E* might be in-plane and out-of-plane vibrational motions of OH and $CO(CH_3)$ groups involved in the H-bonded chelate ring. In fact, the results show active in-plane vibrational modes at 325 and 381 cm^{-1} and out-of-plane motions at 380 cm^{1} which can be correlated to the bands at 307, 365, and 370 cm^{-1}, respectively, observed in the fluorescence excitation spectrum obtained under jet-cooled molecular beam conditions.[23] These correspond to the bending deformations of the H-bond ring. Figure 1 shows a schematic energy profile for the stationary points located at the S_1 state and related structures for the proton-transfer reaction and twisting motion. K* is almost isoenergetic to E*, and the transition state connecting both structures involves an energy barrier of ~5.5 kcal/mol. Rotation of the acetyl group in K* leads to the keto type rotamer KR*. This one is the most stable structure in S_1 (6.23 kcal/mol bellow E*). The protonated acetyl group in KR* is almost perpendicular to the plane defined by the naphthalene ring. After the acetyl group rotation, another transition state (TS_3*) that connects KR* with an equivalent molecular structure was found. While the HAN PES shows three wells with small energy barriers, those of salicylic acid and its methylated derivative (methyl salicylate, MS), another proton-transfer reaction prototype, have been found to have a surface with a single distorted well and, thus, a much more exothermic proton-transfer rection.[36−40] Indeed, K* and E* structures of HAN have almost similar energies contrary to those of MS. These factors play a central role in the surfaces crossing of reactive (π,π^*) and nonreactive (n,π^*) states and, thus, on the spectroscopy and dynamics of proton-transfer reactions and subsequent issues.

In conclusion for this part, the calculations suggest a ground-state PES with two wells corresponding to the enol form (the most stable structure) and to a keto type rotamer. At S_1, a proton-transfer reaction takes place in E* through or over a small barrier of energy to produce a keto type phototautmer. This one may give a keto type rotamer structure which emission should be observed at the red side of the enol and keto emissions. Therefore, the PES at S_1 contains three minima.

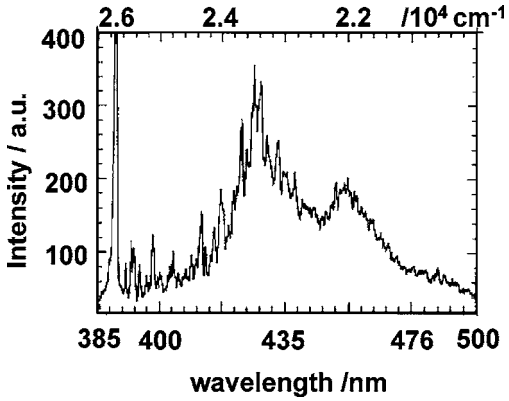

FIGURE 2. Dispersed fluorescence spectrum of a jet-cooled molecular beam of HAN excited at the origin of S_0-S_1 transition (25 735 cm^{-1}, ~389 nm).

Jet-Cooled Molecular Beam Studies

In a supersonic jet-cooled molecular beam of HAN, the dispersed fluorescence indicates the presence of a single conformer at the S_0, state which corresponds to E.[23,24] The excitation of HAN at ~389 nm (S_0-S_1 transition) gives a structured emission which corresponds to that of E* form and two emission bands from the keto type structures with maxima at 426 and 452 nm (Figure 2). The OH/OD isotopic substitution abnormally suppresses the structured emission of E* due to the change in the coupling between the vibrational modes of the involved structures (E* and K*). The isotope effect shows also a tunneling mechanism for the proton transfer in E*. No emission from E* was observed at excess energies of excitation above ~300 cm^{-1}, providing experimental evidence for the existence of an energy barrier (~0.9 kcal/mol) for the proton transfer in the potential energy surface at S_1. In addition to that, the excitation spectrum showed peaks at 203 cm^{-1} and 677 cm^{-1} which might be correlated with the theoretically

observed modes at 189 and 539 cm^{-1}, respectively. These are assigned to the C−O−H out-of-plane mode and the in-plane bending motion of the C═O group, respectively. The bending of this part in the chelate ring induces a variation of the O···O distance and therefore can be considered as an efficient active mode in the proton-transfer dynamics of HAN.[23] Similar observations have been reported in methyl salicylate [15,36−40]. For 2-hydroxyacetophenone (OHAP), a molecule comparable to that of HAN, the bending mode of C═O in the resonance Raman spectrum of OHAP in cyclohexane solutions was observed at 622 cm^{-1}.[41] Immediately after an electronic excitation, and during the time probed by the Raman spectrum, the system evolves along a larger number of vibrational coordinates (appearing in the resonance Raman spectrum) which do not include proton motion.[41] The changes in acidity/basicity character of the involved partners in a proton (or H-atom) motion is governed by a fast electronic redistribution and must occur in the subpicosecond time scale. Therefore, the time scale for proton transfer in HAN will be mainly dictated by the relatively slower in-plane and out-of-plane motions of the H-bonded chelate ring. Oscillations in the femtosecond transmission transient of HAN in cyclohexane were observed with frequencies at 312 and 370 cm^{-1} and assigned to skeletal deformation occurring in the normal modes of the photoproduct after an ultrafast (30 fs) proton motion.[28]

Furthermore, the calculations for HAN suggest that the high activity of the O−H out-of-plane motion (bending mode at 822 cm^{-1}) in E* can suppress the emission signal in the molecular beam beyond ~900 cm^{-1} from the origin of excitation. The fluorescence lifetime of HAN in the molecular beam is 9.4 ns at zero point level of excitation, and it is independent of the observation wavelength, suggesting an equilibrium between E* and K* structures. On the basis of the structured and abnormally shifted emission band of the keto tautomers, the ground-state potential-energy surface has been suggested to contain an additional minimum, which following the theoretical results corresponds to that of keto type rotamers (KR). Using femtosecond time-resolved multiphoton ionization spectroscopy, the ultrafast dynamics of HAN at S_1 pumping at different excitation wavelengths 385−410 nm has been studied.[26] An unresolved fast initial decay followed by a longtime nonexponential decay with two components, $\tau_1 \sim 61-86$ ps related to the proton-transfer process and $\tau_2 \sim 610-1010$ ps assigned to the emission of K* structure, was reported.[26] The results were explained on the basis of an equilibrium between E* and K* with the keto tautomer crossing a very low energy barrier (~0.9 kcal/mol) at the S_1 state. Other gas-phase experiments using time-resolved photoelectron spectroscopy have observed two transient bands in the spectrum of excited HAN and assigned to the photionization of E* and K*.[27] The report also concluded that proton transfer occurs within 50 fs and that the depletion of K* via internal conversion ($S_1 \rightarrow S_0$) occurs in 30 ps, enhanced by a close-lying n,π^* state. Because of the large excess of energy of the pump (>2500 cm^{-1}), the experiment could not detect the small energy barrier for the proton-transfer process (~0.9 kcal/mol).

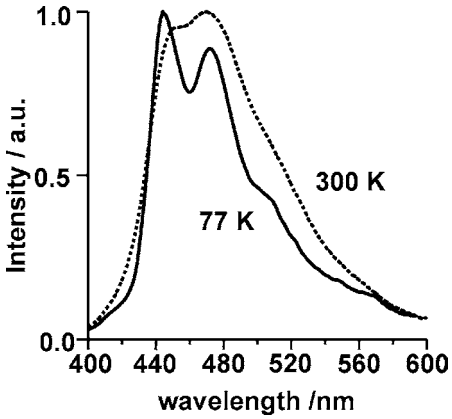

FIGURE 3. Emission spectra of HAN in methyl cyclohexane (MC) at 298 (dotted line) and 77 K (solid line) when excited at 380 nm.

In conclusion for this part, the excited enol structure of HAN in a jet-cooled molecular beam undergoes a fast proton transfer through (tunneling) or over a small barrier of energy. The emission of E* is observed when the excess of the excitation energy is null and vanishes when the excitation is 300 cm^{-1} above the 0−0 transition. Above 900 cm^{-1}, an efficient nonradiative channel is open suppressing the total emission of HAN in the molecular beam. The structured and triple fluorescence bands of HAN suggest that the potential-energy surface at S_1 contains three wells in agreement with the theoretical results.

Temperature Effect Studies

The emission behavior of HAN in solutions at different temperatures has been studied.[34] In methyl cyclohexane (MC, an inert solvent) at 298 K the spectrum band is broad with the maximum at ~480 nm and a shoulder at ~450 nm (Figure 3). At 77 K, the emission exhibits a structured band with maxima at ~440 and ~480 nm. The structural difference between both spectra is due to the involvement of a twisting motion in the formed phototautomer K* to give KR* at S_1. Results of nanosecond−microsecond time-resolved experiments in solution and in rigid media concluded that following the proton-transfer process at S_1 a conformational change takes place in K* to produce a metastable state (keto type rotamer, KR*).[25] Furthermore, a twisting motion in the keto type structure, K*, has been also observed in the proton-transfer cycle of 3′,4′-benzo-2′-hydroxychalcone, a derivative of HAN.[41] A previous report[43] concluded the absence of proton transfer in excited HAN in contrast with others.[23−34] Interestingly, the emission bands of keto structures (with maxima at 440 and 480 nm) at 77 K (Figure 3) might be correlated to those found in cooled molecular beam (maxima 426 and 452 nm) and assigned also to keto phototautomers (Figure 2). The coldest conditions (a few Kelvins) in the supersonic molecular beam experiment and the absence of solvation in these conditions might be the reasons for the blue shift of these emission bands when compared to the 77 K experiment using methylcyclohexane.

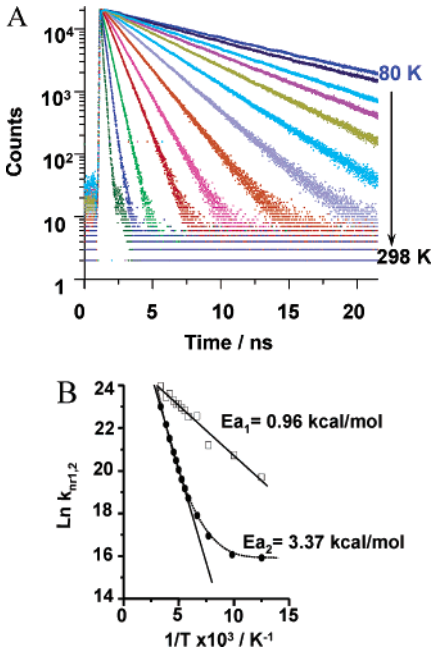

FIGURE 4. (A) Emission decays of HAN in MC at 298, 260, 240, 220, 210, 200, 190, 180, 170, 160, 150, 130, 100, and 80 K when excited at 393 nm and gated at 480 nm. (B) Arrhenius plot (solid line) of the nonradiative rate constants ($k_{nr1,2}$) of HAN in MC vs 1/*T*. E_{a1} and E_{a2} are the activation energies for the nonradiative processes of K* and KR*, respectively. The dotted line indicates the deviation from the Arrhenius behavior.

More information on the effect of the temperature on the photodynamics of HAN in MC was obtained (Figure 4A). The decay fitting at 298 K needed a biexponential function with time constants of 39 ps (22%) and 101 ps (78%). The shortest time constant is assigned to K*, while the longest one is assigned to KR*. Femtosecond experiments in solution showed that the time constant of the proton transfer in E* is ~30 fs.[28] Down to 80 K, the global emission decays show a remarkable change. At 480 nm for example, the lifetime values change from 39 ps to 2.16 ns (4%) and from 101 ps to 8.38 ns (96%) assigned for K* and KR*, respectively. The presence of efficient nonradiative processes at higher temperatures such as those due to twisting along the naphthyl−$COCH_3$ bond, torsion and out-of-plane motion of the naphthalene molecular frame in K* and in KR*, respectively, is the reason for short lifetimes at room temperature. A loss of aromaticity of the naphthalene ring and a lower conjugation with the twisted and protonated acetyl group in KR* have been suggested by theory.[30] Similar emission deactivation processes with a dependency on the viscosity and polarity of the medium have been observed in methyl salicylate.[35]

From the nonradiative decay rate constants of each structure at different temperatures, the activation energies for the radiationless processes for both emitting structures have been deduced (Figure 4B).[34] The activation energy and the frequency factor for nonradiative decays of K* and KR* are $E_{a1} = 0.96 \pm 0.20$ kcal/mol, $A_1 = 9.7 \times 10^{10}$ s^{-1} and $E_{a2} = 3.4 \pm 0.2$ kcal/mol, $A_2 = 2.3 \times 10^{12}$ s^{-1}, respectively. The twisting motion of the protonated acetyl group has a lower energy barrier and a lower frequency term ($A_2/A_1 = 24$) than those of the out-of-plane (dragging) motion of the naphthalene skeleton. In the 298−130 K range the linearity of both plots (Arrhenius type) shows that the nonradiative processes of K* and KR* in MC are controlled by hydrodynamics factors, while below 130 K the deactivation of KR* is rather controlled by free volume factors. In fact, the large solute motions largely decrease while friction and restriction of the solvent motions increase at lower temperatures.[34]

The finding in studying the temperature effect is a large influence of the temperature on the photodynamics of HAN in solution, indicating the large activity of radiationless modes at higher temperatures and identified as twisting motions of the acetyl group and of the naphthalene molecular frame.

Solvent Effects Studies

The effect of the viscosity and hydrogen-bonding interactions of the medium on the deactivation processes of HAN have been studied by recording the fluorescence spectrum and lifetime in different alcohols.[34] In these solvents, the emission decays were fitted using a double-exponential function.[34] For example in methanol, the lifetimes are 34 ps (33%) and 142 ps (67%), while in 1-octanol these times are 63 ps (29%) and 283 ps (71%). The rate constant values of the nonradiative processes, k_{nr}, of both keto phototautomers decrease when the viscosity of the medium increases. The contribution of the short-time component (assigned to K*) drastically decreases when gating the emission at longer wavelengths. For example in 1-butanol, the contribution shows the following changes: 59% (425 nm); 33% (460 nm); 9% (520 nm); 3% (560 nm). Therefore, the emission of K* is centered at the blue part of the spectrum, in full agreement with the temperature and nanocavities results.[31−34] The dependence of the lifetimes of K* and KR* on the viscosity (and polarity; vide infra) of the alcohol series is due to the twisting motions involving the acetyl group and the naphthalene molecular frame in these forms, respectively.

The longest component of the Debye relaxation time τ_D has been used to analyze the nonradiative processes of K* and KR*. Both $k_{nr1,2}$ values decrease when τ_D increases. Thus, a longer Debye relaxation time for solvation shell allows stronger fluorescence of the phototautomers. The solvent friction is more significant for K* (k_{nr1}) than for KR* (k_{nr2}). For the later, the dependence is very weak. This suggests also that motion of the naphthalene ring does not play a major role in the deactivation process of K* and KR*. The result showed also that solvent friction due to hydrogen-bonding interactions between solvent molecules and the phototautomers plays a significant role in the nonradiative processes of both structures.

Both proton transfer and rotation processes involve a charge redistribution, and therefore, a solvent polarity effect is expected. Therefore, solvent effect has been also analyzed by considering the reaction dielectric field factor parameter $f(\epsilon,n) = (\epsilon - 1)/(\epsilon + 2) - (n^2 - 1)/(n^2 + 2)$. For both keto type tautomers, we observed a linear correla-

tion.[34] The results suggests that that the emission of K* in the alcohols family is more efficiently deactivated by solvent polarity than that of KR*. One of the deactivation channels is that of the protonated acetyl rotation in K* leading to KR*. For the alcohols, the viscosity of the medium and the H-bonding interactions with the solute play a crucial role in the deactivation process. Therefore, to reduce the effect of H-bonding donating of the solvent, and working under lower and similar viscosities, the variation of $k_{nr1,2}$ with that of $f(\epsilon,n)$ in nonhydroxylic solvents was examined. Both $k_{nr1,2}$ values decrease when $f(\epsilon,n)$ increases, contrary to the alcohols behavior. This reflects the role played by the H-bonds in the alcohol frictions, making slower the rupture of the clusters structure (solvation shell) around the dye. The dependencies for both $k_{nr1,2}$ in this series of solvents are similar suggesting that the radiationless channel sensitive to polarity is of the same nature for both tautomers. This channel might be connected to the coupling between the π,π^* and n,π^* states mediated out-of-plane motions, as it has been suggested for other comparable systems.[39,40] Therefore, this internal conversion should be more important for K* relaxation leading to shorter lifetimes as it was observed. This reflects the importance of the H-bond between the solvent molecules involved the solvation shell surrounding the dye.

In summary for the neat solvent part, the K* → KR* reaction is dependent on the viscosity, H-bonding, and polarity of the medium. For the alcohols family, the nonradiative rate constants of both keto forms increase with the solvent polarity, while for non-H-bonding media, the reverse trend was observed.

Nanocavity Studies

Caging a molecule into a molecular pocket (nanochamber) produces a confined system with interesting physical and chemical proprieties. It reduces the degrees of freedom available to the molecule to move along the reaction coordinates and confines the wave packet in a small area of propagation.[44] By reduction of the space for relaxation, it makes the system robust and immune to transferring "damage" or heat over long distances. Using ultrafast techniques and selecting the size and nature of the molecular chamber offered by the host to the guest, one will be able therefore to explore and control the spectroscopy (space domain) and dynamics (time domain) in real time of witness.[45,46] Even for small solvent molecules (including water), confinement in nanoporous materials leads to important restriction in the orientational and translational dynamics.[47−50]

In the present case, we will recount the results of the solution nanocavity studies of HAN using cyclodextrins (CD) as host media.[31−33] α-, β-, and γ-CD having large diameter $d \sim 6$, 8.5, and 9.5 Å have been used for nanocaging. Addition of CD's to a water solution of HAN results in an intensity enhancement and shift of the emission band of keto phototautomers. Both observations show the formation and emission behavior of inclusion

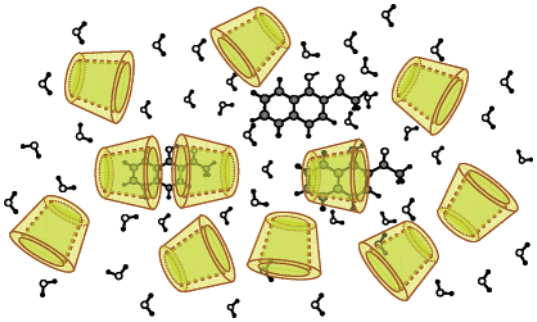

FIGURE 5. Schematic illustration of HAN in water and complexed with one α-, β-, and γ-CD or two α-CD cavities.

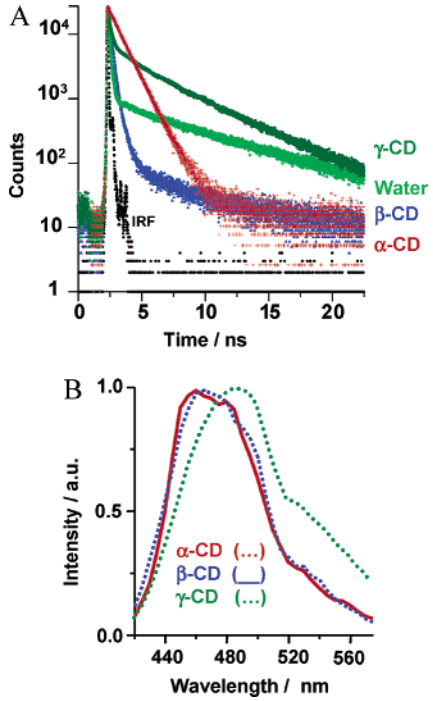

FIGURE 6. (A) 480-nm emission decays of HAN in water and in the presence of mM α-, β-, and γ-CD. (B) Emission spectra of HAN complexed to CD's.

complexes of HAN with the used CD. The stoichiometry of the complexes depends on the nature and size of the cage. For β- and γ-CD, the complex has an 1:1 stoichiometry, while, for α-CD, the stoichiometry is 1:2 HAN:α-CD (Figure 5). Thus, the spectroscopy and dynamics of the complexes have been also found to depend on the nature of the cage (Figure 6). Compared to the observation using water or tetrahydrofuran (considered as a solvent with a polarity comparable to that of CD), the following picture has been provided. Due to the restriction offered by α- and β-CD cages, the rotation of the protonated acetyl group of the guest is restricted giving rise to a stronger K* emission with the maximum in intensity at 460 nm. For γ-CD, a larger cage, the conversion of K* to KR* is allowed; the resulted emission has its maximum at 500 nm, and the phototautomers are more fluorescent due to the protection (from quenchers such as H-bond with water and O_2) provided by the cage. Thus, a shift of ~40 nm is observed, due to an increase in the cavity size of the host. The lifetime of caged KR* is in the nanosecond

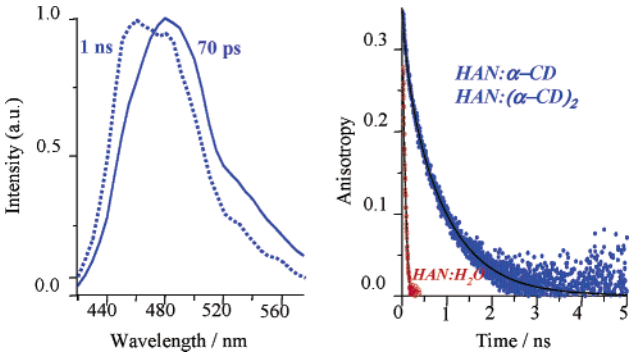

FIGURE 7. Right: Anisotropy decays of HAN in water and in the presence of 10 mM α-CD. The solid lines are the best fits using single or biexponential function. Left: 70-ps and 1-ns gated emission spectra of HAN in the presence of 10 mM α-CD.

regime, while that of caged K* is in the subnanosecond or nanosecond time scale. Depending on the size of CD, the protonated acetyl group can be found inside or outside the cage. So, its twisting to produce KR* and connecting with noradiative channels depend on the degree of confinement and stoichiometry of the complex (Figure 6). The reorientation times of the guest and of the overall guest:host complexes have been examined using anisotropy experiments. To begin with, in pure solvents, like water and tetrahydrofurane, the rotational times are 70 and 35 ps, respectively. These values reflect the role of H-bonding of the solvent (water) and the involvement of the solvation shell (water molecules) in the friction dynamics of the dye. For 1:1 complexes involving β-CD and γ-CD nanocages, this time is 70 and 47 ps, respectively. Thus, for the guest trapped into β-CD ($d \sim 8.5$ Å) the internal molecular rotation is restricted and its time is longer, while included into a larger cavity (γ-CD, $d \sim 9.5$ Å) the internal rotation produces a caged KR* rotamer. The overall rotational time of the complex (HAN:CD) increases with the size of the caging entity: 745 ps and 1.1 ns for β-, and γ-CD complexes, respectively. For, α-CD complexes the situation is different due to the 1:1 and 1:2 (HAN:α-CD) complexes formation involving one or two H-bonded linked CD cavities. Caged and photoproduced K* in 1:1 complexes have the maximum of emission at 480 nm and a lifetime, ∼90 ps, similar to that of free K* in water. Those of the 1:2 complexes are 440 nm and ∼1 ns, respectively (Figure 7). For 1:1 entity, the protonated acetyl group of K* is found outside the CD cavity and it should not suffer any restriction for twisting to produce caged KR* (which was observed). However, for 1:2 complexes, physical restriction dictated by the cavity of 2 linked CD does not allow the formation of KR*, but it enhances the nanosecond emission of caged K*, as this fluorophore is now protected from quenchers and twisting noradiative processes. The $COHCH_3$ rotation in K* to produce KR* involves an energy gain of ∼4 kcal/mol, close to the obtained energy gap (∼6 kcal/ mol) between these structures in gas phase using theoretical calculations. The rotational time of the caged phototautomers into α-CD cages depends on the emission wavelength, and it varies from 50 to 180 ps (Figure 7). That of the global rotational time of 1:2 complex is almost constant, ∼950 ps. This variation with the wavelength of emission indicates the existence of several rotors (or excited conformers) and thus agrees with the involvement of 1:1 and 1:2 complexes. Clearly, the result indicates that the size of the nanocavity of the host governs the emission spectroscopy (space domain, shift by about 40 nm) and the photodynamics (time domain, change from picosecond to nanosecond regime) of the nanostructure.

The experimental observation using CD nanocavities clearly showed the involvement of twisting motion in the formed tautomer K* in the PES of HAN at S_1 and the possible formation of a keto rotamer KR* emitting at the red side of the spectrum. The internal twisting motions and related photophysics can be controlled by choosing the size of the caging nanocavity, a result in full agreement with the calculations, temperature, and solution experiments recounted above.

Conclusion

This Account shows the rich spectroscopy and dynamics of a conceptually simple aromatic molecule bearing two H-bonding groups able to reach, following a photoinduced excitation, an electronic configuration to exchange a proton (or hydrogen atom) in an already formed H-bond at the ground state. The ultrafast shift of the proton (less than 30 fs in solution) might be followed by a twisting motion of the now protonated acceptor group giving birth to an excited keto type rotamer. The radiationless processes of both keto phototaumers are largely sensitive to solvent properties: polarity; H-bonding ability; viscosity. The use of a nanohost like that provided by cyclodextrins is a simple tool to tune the spectroscopy and photodynamics of HAN. We believe that the results and conclusions reached from the studies of HAN in gas, liquid, and cyclodextrin nanocavities, in addition to the theoretical work, are relevant for a better understanding of the behavior of several molecular systems undergoing this kind of phenomena: H-bond rupture within this prototype molecule and subsequent twisting motion are reminiscent to key reactions of chemical bonds governing the architecture, stability, function, and reactivity of many biological systems where charge transfer, proton transfer, twisting motion, and folding are events happening almost continuously at least in living organisms.

I wish to thank my co-workers, who made possible the results recounted here. This work was supported by the MCYT and the JCCM (Spain) through Projects MAT-2002-00301 and PAI-02-004, respectively.

References

(1) Zewail, A. H. The Birth of Molecules. *Sci. Am.* **1990**, *263*, 76.
(2) Zewail, A. H. *Femtochemistry-Ultrafast Dynamics of the Chemical Bond*; World Scientific: River Edge, NJ, Singapore, 1994; Vols. I and II.
(3) *Femtochemistry & Femtobiology: Ultrafast Reaction Dynamics at Atomic-Scale Resolution*; Sundström, V., Ed.; World Scientific: Singapore, 1997.
(4) *Chemical Reactions and Their Control on the Femtosecond Time Scale*; Gaspard, P., Burghardt, I., Eds.; Advances in Chemical Physics 101; Wiley: New York, 1997.

(5) *Femtosecond Chemistry*; Manz, J., Wöste, L., Eds.; VCH: Weinheim, Germany, 1995; Vols. I and II.
(6) *Ultrafast Processes in Chemistry and Biology-Chemistry for the 21st Century*; El-Sayed, M. A., Tanaka, I., Molin, Y. N., Eds.; IUPAC; Blackwell Scientific: Oxford, U.K., 1994.
(7) *Femtosecond Real-Time Spectroscopy of Small Molecules & Clusters*; Schreiber, E., Ed.; Springer: New York, 1998.
(8) *Femtochemistry*; De Schryver, F. C., De Feyter, S., Schweitzer, G., Eds.; Wiley-VCH: Weinheim, Germany, 2000.
(9) *Femtochemistry and Femtobiology, Ultrafast Dynamics in Molecular Science*; Douhal, A., Santamaría, J., Eds.; World Scientific: Singapore, 2002.
(10) Caldin, E. F.; Gold, V. *Proton-Transfer Reactions*; Chapman and Hall: London, 1975.
(11) Barbara, F. P.; Walker, G. C.; Smith, T. P. Vibrational Modes and the Dynamics Solvent Effect in Electron and Proton Transfer. *Science* **1992**, *256*, 975−981.
(12) Douhal, A.; Kim, S. K.; Zewail, A. H. Femtosecond Molecular Dynamics of Tautomerization in Model Base Pairs. *Nature* **1995**, *378*, 260−263.
(13) Stenger, J.; Madsen, D.; Dreyer, J.; Nibbering, E. T. J.; Hamm, P.; Elsaesser, T. Coherent Response of Hydrogen Bonds in Liquids Probed by Ultrafast Vibrational Spectroscopy. *J. Phys. Chem. A* **2001**, *105*, 2929−2932.
(14) Toele, P.; Zhang, H.; Glasbeek, M. Femtosecond Fluorescence Anisotropy Studies of Excited-State Intramolecular Double-Proton Transfer in [2,2′-Bipyridyl]-3,3′-diol in Solution. *J. Phys. Chem. A* **2002**, *106*, 3651−3658.
(15) Su, C.; Lin, J.-Y.; Hsieh, R.-M. R.; Cheng, P.-Y. Coherent Vibrational Motion during the Excited-State Intramolecular Proton-Transfer Reaction in *o*-Hydroxyacetophenone. *J. Phys. Chem. A* **2002**, *106*, 11997−12001.
(16) *Ultrafast Hydrogen Bonding Dynamics and Proton-Transfer Processes in the Condensed Phase*; Elsaesser, T., Bakker, H. J., Eds.; Kluwer Acad. Publishers: Dordrecht, The Netherlands, 2002.
(17) Kompa, K. L.; Levine, R. D. A Moleuclar Logic Gate. *Proc. Natl. Acad. Sci. U.S.A.* **2001**, *98*, 410−414.
(18) Guallar, V.; Moreno, M.; Lluch, J. M.; Amat-Guerri, F.; Douhal, A. H-Atom Transfer and Rotational Processes in the Ground and First Singlet Excited Electronic States of 2-(2′-Hydroxyphenyl)ozaxole Derivatives: Experimental and Theoretical Studies. *J. Phys. Chem.* **1996**, *100*, 19789−19794.
(19) Douhal, A.; Amat-Guerri, F.; Acuña, A. U. Probing Nanocavities with Proton-Transfer Fluorescence. *Angew. Chem., Int. Ed. Engl.* **1997**, *36*, 1514−1516.
(20) García-Ochoa, I.; Díez López, M. A.; Viñas, M. H.; Santos, L.; Martínez-Ataz, E.; Amat-Guerri, F.; Douhal, A. Probing Hydrophobic Nanocavities in Chemical and Biological Systems with a Fluorescent Proton-transfer Dye. *Chem.—Eur. J.* **1999**, *5*, 897−901.
(21) Roshal, A. D.; Grigorovich, A. V.; Doroshenko, A. O.; Pivovarenko, V. G.; Demchenko, A. P. Flavonols and Crown-Flavonols as Metal Cation Chelators. The Different Nature of Ba^{2+} and Mg^{2+} Complexes. *J. Phys. Chem. A* **1998**, *102*, 5907−5914.
(22) Douhal, A.; Roshal, A. D.; Organero, J. A. Stepwise Interaction, Sodium Ion Photoejection and Proton-Transfer Inhibition in a Crown-Ether and Proton-Transfer Dye. *Chem. Phys. Lett.* **2003**, *381*, 519−525.
(23) Douhal, A.; Lahmani, F.; Zehnacker-Rentien, A. Excited-State Intramolecular Proton Transfer in Jet-Cooled 1-Hydroxy-2-acetonaphthone. *Chem. Phys.* **1993**, *178*, 493−504.
(24) Douhal, A.; Lahmani, F.; Zewail, A. H. Proton-Transfer Reaction Dynamics. *Chem. Phys.* **1996**, *207*, 477−498.
(25) Tobita, S.; Yamamoto, M.; Kurahayashi, N.; Tsukagoshi, R.; Nakamura, Y.; Shizuka, H. Effects of Electronic Structures on the Excited-State Intramolecular Proton Transfer of 1-Hydroxy-2-acetonaphthone and Related Compounds. *J. Phys. Chem. A* **1998**, *102*, 5206−5214.
(26) Lu, C.; Hsieh, R.-M- R.; Lee, I.-R.; Cheng, P.-Y. Ultrafast Dynamics of gas-Phase Excited-State Intramolecular Proton Transfer in 1-Hydroxy-2-acetonaphthone. *Chem. Phys. Lett.* **1999**, *310*, 103−110.
(27) Lochbrunner, S.; Schultz, T.; Shaffer, J. P.; Zgierski, M. Z.; Stolow, A. Dynamics of Excited-State Proton-Transfer Systems Via Time-Resolved Photoelectron Spectroscopy. *J. Chem. Phys.* **2001**, *114*, 2519−2522.
(28) Lochbrunner, S.; Stock, K.; De Waele, V.; Riedle, E. Ultrafast Excited-State Proton Transfer: Reactive Dynamics by Multidimensional Wavepacket Motion. In *Femtochemistry and Femtobiology: Ultrafast Dynamics in Molecular Science*; Douhal, A., Santamaria, J., Eds.; World Scientific: Singapore, 2002; pp 202−212.
(29) Organero, J. A.; García-Ochoa, I.; Moreno, M.; Lluch, J. M.; Santos, L.; Douhal, A. A Theoretical Insight into the Internal H-Bond and Related Rotational Motion and Proton Transfer Processes of 1-Hydroxy-2-acetonaphthone in the S_0 State. *Chem. Phys. Lett.* **2000**, *328*, 83−89.
(30) Organero, J. A.; Moreno, M.; Santos, L.; Lluch, J. M.; Douhal, A. Photoinduced Proton Transfer and Rotational Motion of 1-Hydroxy-2-acetonaphthone in the S_1 State: A Theoretical Insight into Its Photophysics. *J. Phys. Chem. A* **2000**, *104*, 8424−8431.
(31) Organero, J. A.; Santos, L.; Douhal, A. Breaking, Making and Rotating Chemical Bonds of 1′-Hydroxy-2′-acetonaphthone in Solutions and in Nanocavities. In *Femtochemistry and Femtobiology: Ultrafast Dynamics in Molecular Science*; Douhal, A., Santamaria, J., Eds.; World Scientific: Singapore, 2002; pp 225−233.
(32) Organero, J. A.; Tormo, L.; Douhal, A. Caging Ultrafast Proton Transfer and Twisting Motion of 1-Hydroxy-2-acetonaphthone. *Chem. Phys. Lett.* **2002**, *363*, 409−414.
(33) Organero, J. A.; Douhal, A. Confinement Effects on the Photorelaxation of a Proton Transfer Phototautomer. *Chem. Phys. Lett.* **2003**, *373*, 426−431.
(34) Organero, J. A.; Douhal, A. Temperature and Solvent Effects on the Photodynamics of 1′-Hydroxy-2′-acetonaphthone. *Chem. Phys. Lett.* **2003**, *381*, 759−765.
(35) Smith, K. K.; Kaufmann, K. J. Solvent Dependence of the Nonradiative Decay Rate of Methyl Salicylate. *J. Phys. Chem.* **1981**, *85*, 2895−2897.
(36) Felker, P. M.; Lambert, W. R.; Zewail, A. H. Picosecond Excitation of Jet-Cooled Hydrogen-Bonded Systems: Dispersed Fluorescence and Time-Resolved Studies of Methyl Salicylate. *J. Chem. Phys.* **1982**, *77*, 1603−1605.
(37) Helmbrook, L.; Keny, J. E.; Kohler, B. E.; Scott, G. W. Lowest Excited Singlet State of Hydrogen-bonded Methyl Salicylate. *J. Phys. Chem.* **1983**, *87*, 280−289.
(38) Herek, J. L.; Pedersen, S.; Bañares, L.; Zewail, A. H. Femtosecond Real-Time Probing of Reactions. IX. Hydrogen-Atom Transfer. *J. Chem. Phys.* **1992**, *97*, 9046−9061.
(39) Sobolewski, A. L.; Domcke, W. Ab initio Potential-Energy Function for Excited-State Intramolecular Proton transfer: A Comparative Study of o-Hydroxybenzaldehyde, Salicylic Acid and 7-Hydroxy-1-indanone. *Phys. Chem. Chem. Phys.* **1999**, *1*, 3065−3072.
(40) Scheiner, S. Theoretical Studies of Excited-State Proton Transfer in Small Model Systems. *J. Phys. Chem. A* **2000**, *104*, 5898−5909.
(41) Peteanu, L. A.; Mathies, R. A. Resonance Raman Intensity Analysis of the Excited-State Proton Transfer in 2-Hydroxyacetophenone. *J. Phys. Chem.* **1992**, *96*, 6910−6916.
(42) Tokumura, K.; Nagaosa, K.; Matsushima, R. Temperature-Dependent Tautomer Fluorescence Spectra of 3′,4′-Benzo-2′-hydroxychalcone: Direct Evidence for Photoenolization Followed by Z → E Isomerization in the Singlet Manifold. *Chem. Phys. Lett.* **1998**, *195*, 516−524.
(43) Catalán, J.; Del Valle, J. C. Toward the Photostability Mechanism of Intramolecular Hydrogen Bond Systems. Photophysics of 1′-Hydroxy-2′-acetonaphthone. *J. Am. Chem. Soc.* **1993**, *115*, 4321−4325.
(44) Douhal, A. A Quick Look at Hydrogen Bonds. *Science* **1997**, *276*, 221−222.
(45) Douhal, A. Femtochemistry in Nanocavities. In *Femtochemistry*; De Schryver, F. C., De Feyter, S., Schweitzer, G., Eds.; Wiley-VCH: Weinheim, Germany, 2001; Chapter 15.
(46) Zhong, D.; Douhal, A.; Zewail, A. H. Femtosecond Studies of Protein-Ligand Hydrophobic Binding and Dynamics: Human Serum Albumin. *Proc. Natl. Acad. Sci. U.S.A.* **2000**, *97*, 14056−14061.
(47) Nandi, N.; Bhattacharyya, K.; Bagchi, B. Dielectric Relaxation and Solvation Dynamics of Water in Complex Chemical and Biological Systems. *Chem. Rev.* **2000**, *100*, 2013−2046.
(48) Winkler, K.; Lindler, J.; Bursing, H.; Vohringer, P. Ultrafast Raman-Induced Kerr Effect of Water: Single Molecule Versus Collective Motions. *J. Chem. Phys.* **2000**, *113*, 4674−4682.
(49) Bhattacharyya, K. Solvation Dynamics and Proton Transfer in Supramolecular Assemblies. *Acc. Chem. Res.* **2003**, *36*, 95−101.
(50) Farrer, R. A.; Fourkas, J. T. Orientational Dynamics of Liquids Confined in Nanoporous Sol−Gel Glasses Studied by Optical Kerr Effect Spectroscopy. *Acc. Chem. Res.* **2003**, *36*, 605−612.

AR030247B